STEM CELLS®

CANCER STEM CELLS

Sarcoma Derived from Cultured Mesenchymal Stem Cells

JAKUB TOLAR,[a] ALMA J. NAUTA,[b] MARK J. OSBORN,[a] ANGELA PANOSKALTSIS MORTARI,[a] RON T. MCELMURRY,[a] SCOTT BELL,[a] LILY XIA,[a] NING ZHOU,[a] MEGAN RIDDLE,[a] TANIA M. SCHROEDER,[c] JENNIFER J. WESTENDORF,[d] R. SCOTT MCIVOR,[e] PANCRAS C.W. HOGENDOORN,[f] KAROLY SZUHAI,[g] LEANN OSETH,[a] BETSY HIRSCH,[e,h] STEPHEN R. YANT,[i] MARK A. KAY,[i] ALEXANDRA PEISTER,[j] DARWIN J. PROCKOP,[j] WILLEM E. FIBBE,[b] BRUCE R. BLAZAR[a]

[a]Department of Pediatrics, Division of Hematology-Oncology, Blood and Marrow Transplant and Cancer Center, University of Minnesota Medical School, Minneapolis, Minnesota, USA; [b]Department of Immuno-hematology and Blood Transfusion, Leiden University Medical Center, Leiden, The Netherlands; [c]Graduate Program in Biochemistry, Molecular Biology and Biophysics, University of Minnesota Medical School, Minneapolis, Minnesota, USA; [d]Department of Orthopedic Surgery, University of Minnesota Medical School, Minneapolis, Minnesota, USA; [e]Institute of Human Genetics, University of Minnesota Medical School, Minneapolis, Minnesota, USA; [f]Department of Pathology, Leiden University Medical Center, Leiden, The Netherlands; [g]Department of Molecular Cell Biology, Leiden University Medical Center, Leiden, The Netherlands; [h]Department of Laboratory Medicine and Pathology, University of Minnesota Medical School, Minneapolis, Minnesota, USA; [i]Departments of Pediatrics and Genetics, Stanford University School of Medicine, Stanford, California, USA; [j]Tulane School of Medicine, New Orleans, Louisiana, USA

Key Words. Mesenchymal stem cells • Sarcoma • Neoplastic cell transformation • DNA transposable elements Bone marrow transplantation

ABSTRACT

To study the biodistribution of MSCs, we labeled adult murine C57BL/6 MSCs with firefly luciferase and DsRed2 fluorescent protein using nonviral *Sleeping Beauty* transposons and coinfused labeled MSCs with bone marrow into irradiated allogeneic recipients. Using in vivo whole-body imaging, luciferase signals were shown to be increased between weeks 3 and 12. Unexpectedly, some mice with the highest luciferase signals died and all surviving mice developed foci of sarcoma in their lungs. Two mice also developed sarcomas in their extremities. Common cytogenetic abnormalities were identified in tumor cells isolated from different animals. Original MSC cultures not labeled with transposons, as well as independently isolated cultured MSCs, were found to be cytogenetically abnormal. Moreover, primary MSCs derived from the bone marrow of both BALB/c and C57BL/6 mice showed cytogenetic aberrations after several passages in vitro, showing that transformation was not a strain-specific nor rare event. Clonal evolution was observed in vivo, suggesting that the critical transformation event(s) occurred before infusion. Mapping of the transposition insertion sites did not identify an obvious transposon-related genetic abnormality, and p53 was not overexpressed. Infusion of MSC-derived sarcoma cells resulted in malignant lesions in secondary recipients. This new sarcoma cell line, S1, is unique in having a cytogenetic profile similar to human sarcoma and contains bioluminescent and fluorescent genes, making it useful for investigations of cellular biodistribution and tumor response to therapy in vivo. More importantly, our study indicates that sarcoma can evolve from MSC cultures. STEM CELLS *2007;25:371–379*

INTRODUCTION

Adult bone marrow (BM) is a site of origin of several types of hematopoietic and nonhematopoietic stem cells with distinct functions. For instance, MSCs can differentiate into nonhematopoietic cell types, including adipocytes, chondrocytes, and osteocytes. MSCs have been isolated from multiple species, including humans [1–6], and multiple organs, including BM, adipose tissue [7], or umbilical cord blood [8]. The beneficial effects of MSCs are being tested clinically in attempts to improve hematopoietic engraftment [9], to treat osteogenesis imperfecta [10], graft-versus-host disease [11], and autoimmune diseases [12–14], and to deliver therapy for malignancies [15, 16]. In early reports, Phase I clinical studies have not been associated with toxicities.

We aimed to investigate the capacity of MSCs to aid in tissue healing after radiation-induced injury in irradiated allogeneic BM transplant (BMT) recipients. We used *Sleeping Beauty* (SB) transposons [17] to label MSCs with the firefly *luciferase* gene and the sea coral-derived red fluorophore *DsRed2* gene [18] to monitor MSCs in vivo by bioluminescence intensity (BLI) and in tissue sections by emitted fluorescence, respectively. *SB* is a synthetic *Tc1/mariner*-type DNA transposon from salmonid fish which is functional in eukaryotic cells and recognizes specific inverted/direct repeat sequences flank-

Correspondence: Jakub Tolar, M.D., Ph.D., Pediatric Hematology/Oncology/Blood and Marrow Transplant Program, MMC 366, 420 Delaware Street SE, Minneapolis, Minnesota 55455, USA. Telephone: 612-626-5501; Fax: 612-624-3913; e-mail: tolar003@umn.edu
Received December 9, 2005; accepted for publication October 6, 2006; first published in STEM CELLS *EXPRESS* October 12, 2006; available online without subscription through the open access option. 1066-5099/2007/$30.00/0 doi: 10.1634/stemcells.2005-0620

ing a sequence of interest to mediate transposition. Importantly, integration by transposition does not change adjacent host DNA sequences except for the duplication of the target TA dinucleotide. Transposons are relatively easy to produce, have been used successfully for germ-line and somatic transgenesis, and, when compared with viral vectors, may be less immunogenic because no viral proteins are present which may be relevant for clinical application [19–21].

Unexpectedly, in our study, infusion of gene-modified MSCs in vivo was associated with increased mortality and tumors in lungs and extremities. The donor-derived transformed cells were aneuploid, and by histology, the tumors were identified as sarcomas which when infused into secondary recipients produced similar tumors. The original MSC culture not labeled with transposons was found to be cytogenetically abnormal, and the clonal evolution of these cells to sarcomas was observed after in vivo infusion. Additionally, independently isolated primary MSC cultures from BM of two mouse strains displayed abnormal karyotypes in vitro. Taken together, these data, along with mapping of transposition sites in the genome and karyotype analysis, suggested that the critical transformation event(s) occurred before infusion of the MSCs. These findings provide evidence of evolution of murine MSCs into sarcoma in vivo and may be clinically relevant because they document the potential of MSCs for transformation into malignant disease.

MATERIALS AND METHODS

MSC Culture and Labeling

MSCs were isolated from adult, 8- to 10-week-old C57BL/6 mice. Femoral heads and condyles were removed, and BM was collected by centrifugation of the bones at 400*g* for 1 minute. BM was filtered through a 70-nm nylon mesh filter and cultured in MSC media as described previously [6]. Briefly, the cells were plated in complete isolation media (CIM). CIM consisted of RMPI 1640 (Invitrogen Corporation, Carlsbad, CA, http://www.invitrogen.com), 9% fetal bovine serum (Atlanta Biologicals, Lawrenceville, GA, http://www.atlantabio.com), 9% horse serum (HyClone, Logan, UT, http://www.hyclone.com), 100 U/ml penicillin (Invitrogen Corporation), 100 μg/ml streptomycin (Invitrogen Corporation), and 2 μM L-glutamine (Invitrogen Corporation). After 24 hours, nonadherent cells were removed. Adherent cells were washed with phosphate-buffered saline (PBS) and fresh CIM was added every 3–4 days. After 4 weeks in culture, the cells were lifted with 0.25% trypsin/0.53 mM EDTA (Invitrogen Corporation) and plated at 50 cells/cm^2 in complete expansion media (CEM). CEM consisted of Iscove's modified Dulbecco medium (IMDM) (Invitrogen Corporation), 9% fetal calf serum, 9% horse serum, 100 U/ml penicillin, 100 μg/ml streptomycin, and 2 μM L-glutamine. Cells were expanded at low density (50–100 cells/cm^2) in the CEM (replaced every 3–4 days) [6]. MSCs displayed oligopotentiality, morphology, and cell surface antigen expression characteristic of MSCs (data not shown; supplemental online Fig. 1).

For some studies, MSCs were labeled with firefly luciferase and red fluorescent protein DsRed2 using the *SB* transposon system (pT). Transposons are DNA elements that move from one genomic position to another. They are flanked by inverted terminal repeats, which are recognized by a transposase enzyme. *SB* transposon–transposase system mediates gene integration via a "cut-and-paste" mechanism of transposition, resulting in stable transgene integration into host genomic DNA TA dinucleotides. Firefly luciferase was chosen to allow serial assessment of biodistribution and persistence of MSCs in vivo. DsRed2 was chosen as a marker of donor cells in tissue sections, obviating the need for antibody staining. Firefly luciferase and red fluorescent protein DsRed2 were expressed from a chicken β-globin and cytomegalovirus composite promoter (CAGGS), and hyperactive *SB* transposase mutant (HSB2) [22] was expressed from cytomegalovirus promoter (CMV). Two months after isolation from adult C57BL/6 BM (at passage 6), MSCs (1×10^6 cells) were conucleofected (Amaxa Inc., Gaithersburg, MD, http://www.amaxa.com) (setting T-20, buffer T) with 5 μg each of pT/CAGGS-DsRed2 and pT/CAGGS-luciferase, and HSB2 at a 1:50 ratio (0.1 μg of p/CMV-HSB2). To isolate DsRed2$^+$ cells, single-cell suspensions of nucleofected MSCs were prepared in buffer (PBS + 2% bovine serum + 0.15% sodium azide) and 24 hours after nucleofection were sorted for MSCs with the highest 5% of DsRed2 expression using a FACS calibur (Becton Dickinson, Palo Alto, CA).

Mouse Strains

B10.BR mice, nonobese diabetic/severe combined immunodeficient (NOD/SCID) mice, BALB/c, and C57BL/6 mice were obtained from The Jackson Laboratory (Bar Harbor, ME, http://www.jax.org) or from Charles River Laboratories (Maastricht, The Netherlands, http://www.criver.com). All mice were housed under specific-pathogen free conditions, fed ad libitum according to University of Minnesota Research Animal Resources and Leiden University Medical Center Animal Facilities guidelines, and used at 6–12 weeks of age. All protocols involving mice were approved by the Institutional Animal Care and Use Committee.

BMT and Sarcoma Cell Infusions

Donor C57BL/6 BM was T-cell-depleted (TCD) using anti-Thy 1.2 monoclonal antibody (mAb) (clone 30-H-12, rat immunoglobulin $G2_b$ [$IgG2_b$], provided by Dr. David Sachs, Charleston, MA) and complement (Nieffenegger, Woodland, CA). B10.BR mice ($H2^k$) were lethally irradiated with 8.0 Gy by x-ray (0.39 Gy per minute) on the day prior to transplantation of 20×10^6 C57BL/6 ($H2^b$) TCD BM cells alone or with 3×10^6 C57BL/6 luciferase- and DsRed2-expressing MSCs (termed MSC DL, passage 9) on day 0 intravenously via tail vein. In addition, 1.5×10^6 C57BL/6 luciferase- and DsRed2-expressing MSCs were infused on day 3.

For sarcoma cell infusions, tumor cells derived from C57BL/6 MSCs that had not been labeled with transposons (termed B6-T1) were reinjected in C57BL/6 mice at a dose of 1×10^6 cells per mouse. In other studies, C57BL/6 MSCs that were transposon-labeled (termed S1) were injected at a dose of 1×10^6 cells intravenously, intraperitoneally, or intramuscularly into NOD/SCID mice.

In Vivo Imaging of Luciferase Activity and DsRed2 Fluorescence

At 7 and 18 weeks after MSC DL infusion, mice were anesthetized with Nembutal (0.1 ml/10 mg of body weight) and the abdomen and chest were shaven. Luciferin stock (30 mg/ml; Xenogen Corporation, Hopkinton, MA, http://www.xenogen.com) was injected intraperitoneally into the mice at 150 mg/kg. A grayscale reference image was taken of the position of the mice prior to assessing luciferase activity. Bioluminescent signals were assessed at 5 minutes after luciferin injection at an integration time of 1 second to 2 minutes using an in vivo imaging system that uses a cooled charge-coupled device camera (IVIS100; Xenogen Corporation). Pseudocolor images representing the bioluminescent signal intensity (blue is the least intense, and red is the most intense) were superimposed over the grayscale reference image. The scales for the pseudocolor intensity plots are displayed with the images. For DsRed2 fluorescence whole-body imaging, photos of anesthetized mice were taken with a Magnafire color camera (Optronics, Goleta, CA, http://www.optronics.com) mounted onto a Leica MZFLIII stereomicroscope (Leica, Wetzlar, Germany, http://www.leica.com).

Radiographic and Digital Images

Mice were anesthetized as described and placed in a prone position with humeri and femora set perpendicular to the vertebral column. Whole-body radiographs were taken under ×5 magnification using a Faxitron Specimen Radiography System (Model MX-20; Faxitron X-ray Corporation, Wheeling, IL, http://www.faxitron.com). Images were captured on Kodak Min-R 2000 mammography film (Eastman Kodak Co., Rochester, NY, http://www.kodak.com) (ex-

posure settings: 7 seconds, 24 kVp). Computed tomography (CT) images were obtained using a Siemens Volume Zoom 4 scanner (Siemens AG, Munich, Germany, http://www.siemens.com). Macroscopic photos were obtained using a digital camera (Coolpix 4300; Nikon Corporation, Tokyo, http://www.nikon.com).

Pulmonary Function Tests

Where indicated, pulmonary function measurements on anesthetized mice were obtained by whole-body plethysmography using the Flexivent system (SCIREQ Scientific Respiratory Equipment Inc., Montreal, QC, Canada, http://www.scireq.com). Change in transpulmonary pressure required to produce a unit flow of gas through the airways of the lung (resistance: cm H_2O/ml/second) and change in lung volume produced by a given change in transpulmonary pressure (compliance: 1/cm H_20 pressure) were determined.

Tissue Analysis for MSC DL Localization and Differentiation

Tissue specimens of the recipient animals were cryopreserved in optimal cutting temperature medium (Sakura Finetek U.S.A., Inc., Torrance, CA, http://www.sakuraus.com) at −80°C. Six-micrometer-thick cryosections were mounted on glass slides, and fixed in acetone for 5 minutes at room temperature. Cryosections were stained either with hematoxylin-eosin (Sigma-Aldrich, St. Louis, http://www.sigmaaldrich.com) or with nuclear stain 4′,6-diamidino-2-phenylindole (DAPI) (Invitrogen Corporation) and examined for native fluorescence of DsRed2 by confocal fluorescence microscopy (Olympus AX70; Olympus Optical Co., Ltd., Tokyo, http://www.olympus-global.com). For differentiation assays, cells were cultured and stained as described previously [6]. Chondrocyte pellets were stained with anti-collagen II antibody (Spring Bioscience, Fremont, CA, http://www.springbio.com). Evaluation of p53 expression was performed as described previously [23].

In Vitro Quantification of Luciferase Expression

Single-cell suspensions of MSCs or tissue homogenates of organ specimens that had been harvested after centrifugation were assayed for luciferase activity using bioluminescence as follows: cells were harvested by centrifugation, resuspended in 100 μl of culture media with 10 μl of luciferin stock (30 mg/ml; Xenogen Corporation), and assayed immediately for bioluminescence activity on a Chameleon 425-100 Multi-label Counter (Hidex, Turku, Finland, http://www.hidex.com). Average relative luminescence values were expressed as counts per second and for tissue homogenates were further normalized to total protein (Dojindo Laboratories, Kumamoto, Japan, http://www.dojindo.co.jp).

Flow Cytometry of MSCs or Sarcoma Cells

Single-cell suspensions of MSCs or sarcoma cells were prepared in buffer (PBS + 2% bovine serum). Pelleted cells were incubated for 15 minutes at 4°C with 0.4 μg of anti-Fc receptor mAb (clone 2.4G2, rat IgG_{2b}) to prevent Fc binding. Flow cytometry was performed using directly conjugated (fluorescein isothiocyanate) mAb to assess cell surface antigen expression. Optimal concentrations of directly conjugated mAbs were added to a total volume of 100–130 μl and incubated for 1 hour at 4°C. The following mAbs were obtained from BD Pharmingen (San Diego, http://www.bdbiosciences.com/pharmingen): anti-CD11b, anti-CD34, anti-CD45, anti-Ly-6A/E (stem cell antigen-1), anti-CD106 (vascular cell adhesion nolecule-1), anti-CD31 (platelet endothelial cell adhesion molecule), anti-CD90 (Thy-1), anti-CD116, and anti-CD117 (c-kit). All samples were analyzed on a FACS calibur (Becton Dickinson) using Cell Quest software. Forward and 90 degree side-scatter were used to identify and gate the live cell population. A minimum of 10,000 events was examined.

Cell Population Growth Dynamics

MSCs (passage 3 and passage 8) and tumor cells (S1 and S2) were plated in duplicate at varying densities (50, 100, and 500 cells/cm^2) on 150-cm^2 plates in CEM. Cells were grown in a 37°C, 5% CO_2 incubator, and the medium was changed every 2 days for a total of 12 days. The cells were lifted with 0.05% trypsin/0.53 mM EDTA (Invitrogen Corporation), and cells from each plate were counted every 3 days for 12 days with a hemacytometer (Vi-CELL Series Cell Viability Analyzer; Beckman Coulter, Fullerton, CA, http://www.beckmancoulter.com).

Cytogenetic Analysis

After a 3.5-hour Colcemid treatment, cells were harvested according to standard cytogenetic techniques involving hypotonic treatment in 0.75 M KCl and fixation in 3:1 methanol/acidic acid. The resulting metaphase cells were evaluated by G-banding. The G-banded interpretation of the karyotype was refined and confirmed by fluorescence in situ hybridization (FISH) with spectral karyotyping (SKY). Slides were prepared for SKY using standard technique (Applied Spectral Imaging Inc., Vista, CA, http://www.spectralimaging.com). SKY metaphases were visualized using a SKY filter and captured and karyotyped using SkyView software (Applied Spectral Imaging Inc.). For some samples, the mouse multicolor FISH was performed by the combined binary ratio (COBRA) approach as previously described [24]. Mouse whole-chromosome libraries were kindly provided by Dr. Michael Speicher (Graz, Austria). The 21 whole-chromosome DNA sets were amplified by degenerate-oligonucleotide priming polymerase chain reaction (PCR) [25, 26] and labeled by the Universal Linkage System labeling systems (ULS) (Kreatech Biotechnology B.V., Amsterdam, The Netherlands, http://www.kreatech.com), diethyl aminomethyl coumarin (DEAC), cyanine 3 (Cy3), and Cy5 as ratio-fluorochromes to generate color images (red, green, blue), whereas the odd-numbered chromosomes and the Y chromosome were additionally labeled by combinatory approach using rhodamine green ULS reagent. The hybridization conditions and posthybridization washes were performed according to published protocols [24]. Slides were counterstained with DAPI immersed in antifading solution (Citifluor; Agar Scientific, Stansted, U.K., http://www.agarscientific.com). Digital fluorescence imaging was performed using a Leica DM-RXA epifluorescence microscope (Leica) equipped with a computer-controlled filter rotor with excitation and emission filters for visualization of DAPI, DEAC, fluorescein (for visualization of rhodamine green), rhodamine (for visualization of Cy3), and Cy5. Image analysis was done using the COBRA-FISH software as described previously [27]. For each sample, at least 20 metaphases were analyzed with regard to structural rearrangements and general ploidy level.

Western Blotting for SB Transposase Protein

For western blotting, 20 μg each of sarcoma-derived cell lysates, or HSB2-transfected cells as a control, were separated on a 10% Bis-Tris NuPAGE gel using the XCell SureLock Mini-Cell following the manufacturer's instructions (Invitrogen Corporation). Protein transfer to a polyvinylidene difluoride membrane was accomplished using the Xcell II Blot Module (Invitrogen Corporation). The blot was probed with a rabbit polyclonal anti-SB transposase antibody followed by addition of horseradish peroxidase-conjugated anti-rabbit IgG (GE Healthcare, Little Chalfont, Buckinghamshire, U.K., http://www.gehealthcare.com) and developed using the ECL Western Blotting Analysis System (GE Healthcare).

Quantitative Real-Time PCR and Alkaline Phosphatase Enzyme Assays

Total RNA was isolated from MSCs and S1 cells using TriZol reagent (Invitrogen Corporation). Reverse transcription of total RNA into cDNA and real-time PCR were performed in one step using the QuantiTect SYBR Green RT-PCR kit (Qiagen Inc., Valencia, CA, http://www1.qiagen.com) and a Lightcycler (Roche Diagnostics, Indianapolis, http://www.roche-diagnostics.com). Primers specific for osteopontin, bone sialoprotein, osteocalcin, and actin were previously described [28]. Quantitative real-time PCR analyses and alkaline phosphatase assays were performed as previously reported [28].

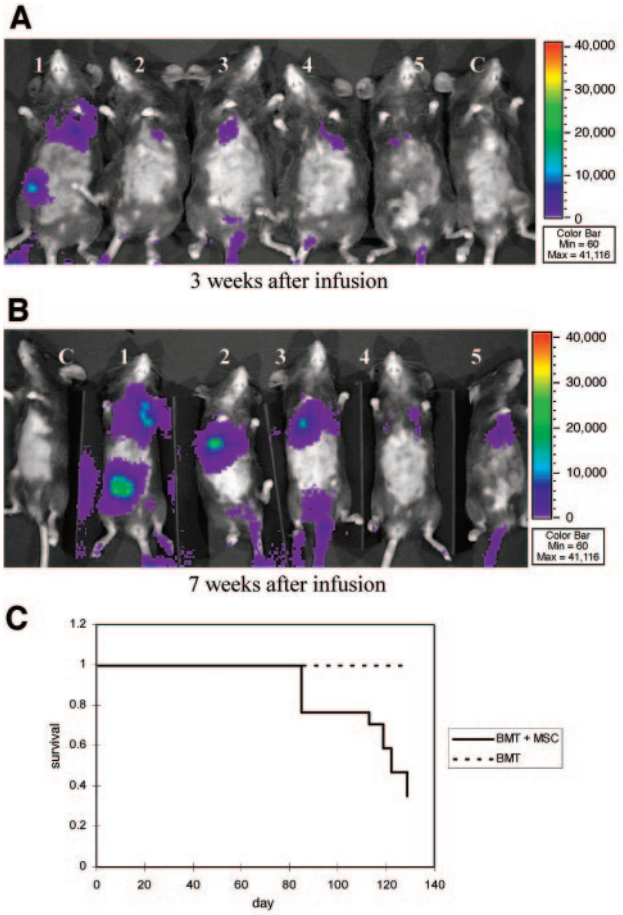

Figure 1. Ex vivo modified MSCs are associated with increased mortality. **(A):** Whole-body bioluminescent imaging performed at 3 weeks. Five representative animals (out of 17) are shown. Exposure time, 2 minutes. **(B):** Whole-body bioluminescent imaging performed at 7 weeks. Bioluminescence intensity (BLI) signals detected over upper thorax increased between 3 and 7 weeks after infusion in most mice (the same five representative animals out of 17 are shown; 0.7-fold to 158-fold increase of maximum BLI signals; $p = .039$). Exposure time, 2 minutes. The control animal (C) was untreated. **(C):** Late-onset mortality was observed in recipients of MSC DsRed2 and luciferase positive + BMT but not in recipients of BMT alone ($p < .01$). Abbreviation: BMT, bone marrow transplantation.

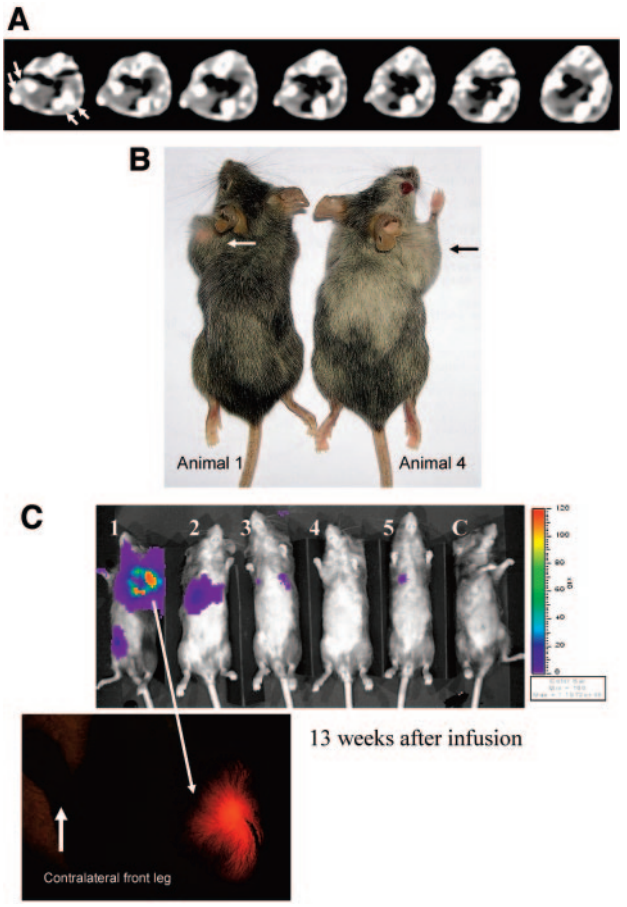

Figure 2. Lung and extremity tumors develop in recipients of DsRed2 and luciferase positive MSC (MSC DLs). **(A):** Ectopic ossicles (arrows) were found using computed tomography in the lungs of all animals that were infused with MSC DLs and bone marrow transplantation (BMT) (seven optical sections of one representative animal are shown). **(B):** At 15 weeks after MSC DL infusion, 2 of 17 recipients of MSC DL + BMT developed soft-tissue tumors (arrows). **(C):** The tumor in one animal (animal 1) was luciferase$^+$ (top panel) and DsRed2$^+$ (bottom panel), whereas the macroscopically similar tumor in the other animal (animal 4) was luciferase$^-$ (top panel) and DsRed2$^-$ (data not shown). Color bar: Min = 100, Max = 11,972. Exposure time, 2 minutes. Abbreviation: C, control animal.

Data Analysis

Differences between measurements were assessed using Fisher's exact test, with p value $< .05$ considered significant.

RESULTS

Lung Ectopic Ossicles and Lung Function

To assess the distribution of MSC DLs (DsRed2$^+$, luciferase$^+$ MSCs) in vivo, B10.BR mice were lethally irradiated and given C57BL/6 TCD BM cells alone or with MSC DLs (passage 9) on day 0 and day 3 after BM infusion. In vivo whole-body imaging was performed every 2 weeks. BLI signals detected over the upper thorax increased between 3 and 7 weeks after infusion in most mice (Fig. 1A, 1B, five animals representative of all 17 are shown; 0.7-fold to 158-fold increase of maximum BLI signals; $p = .039$).

Three animals died at approximately week 12, two of which exhibited high levels of luciferase expression by BLI measured in the area from the shoulders to the mid-abdomen of each mouse (data not shown). Seven more MSC DL recipients died by the end of the experiment 18 weeks post-transplant, resulting in a significantly lower survival rate in BMT recipients given MSC DLs versus those receiving BMT alone ($p < .01$; Fig. 1C).

To assess the cause of death and because the location of the BLI signals indicated a high intensity in the chest, we performed chest CT scans of the remaining animals at 14 weeks post-transplant. CT scans showed ectopic ossicles (two to eight per mouse) in the lungs of all 12 surviving BMT recipients infused with MSC DLs (Fig. 2A). All 17 animals died prematurely and/or developed tumors. Notably, tumors were found in all animals, even those that experienced a decrease in the luciferase signals, presumably as a result of silencing of the luciferase reporter gene expression as documented for the sarcoma line termed S2 and as described below. No foci of ectopic ossification were noted in the lungs of the animals that received conditioning and BM only ($n = 10$; data not shown).

Ectopic lung ossicles occupied substantial space in the thoracic cavity. To determine the degree to which the ossicles

compromised lung function, pulmonary function tests (PFTs) were performed in recipients of MSC DLs + BMT ($n = 4$). Change in transpulmonary pressure required to produce a unit flow of gas through the airways of the lung (resistance) and change in lung volume produced by a given change in transpulmonary pressure (compliance) were measured and the results were compared with PFTs of control cohort recipients of BMT alone ($n = 3$). Significant differences were evident in BMT alone versus BMT + MSC DL recipients with increased resistance (average ± standard deviation, 0.65 ± 0.08 vs. 0.92 ± 0.12 cm H_20/ml per second; $p = .018$) and decreased compliance (0.028 ± 0.005 vs. 0.018 ± 0.005 1/cm H_20 pressure; $p = .038$), consistent with restrictive pulmonary disease of a sufficient severity to have likely contributed to the observed late-onset mortality.

Extremity Sarcomas

In addition to ectopic ossicles in the lungs, readily visualized tumors in forelegs, histologically classified as sarcoma, were noted in two of 17 mice studied at 15 weeks after infusion of MSC DLs and BM (Fig. 2B). Cells derived from the extremity tumor of animal 1, termed S1 (Figs. 1B, 2B, 2C), emitted luciferase bioluminescence and DsRed2 fluorescence, whereas cells derived from the extremity tumor of animal 4, termed S2, did not (Figs. 1B, 2B, 2C). To more completely assess the biology of these tumors, all mice were sacrificed 18 weeks after BMT to permit tissue analysis and to isolate cell lines. Lesions in the extremity and lung were calcified (Fig. 3A, 3B). Tumor histology evaluated by light and electron microscopy was consistent with osteosarcoma: tumors consisted of dense sheets and fasciculi of spindloid cells with widespread deposition of a homogenous eosinophilic substance (osteoid) in a trabecular pattern (Fig. 3C). DsRed2$^+$ progeny of donor MSC DL cells were detected in lung lesions and S1 tumor line derived from animal 1 (Fig. 4A, 4B) but not in the lung lesions or S2 tumor derived from animal 4 (Fig. 4C). There was no spread of S1 or S2 to liver, spleen, kidney, heart, brain, or BM as assessed by in vitro luciferase assay in tissue homogenates and by macroscopic and microscopic examination (data not shown).

In Vitro Growth and Differentiation and In Vivo Metastatic Potential of Sarcoma Cells

Cells from the S1 sarcoma appeared strikingly different from the original MSCs. As compared with passage 3 MSCs, S1 cells were larger, divided rapidly (population growth dynamics are shown in supplemental online Fig. 2), and displayed minimal contact inhibition (supplemental online Fig. 3). In contrast to MSCs, which displayed oligopotentiality, S1 cells could be induced in vitro to differentiate into osteocytes but not adipocytes or chondrocytes (supplemental online Fig. 3). Sarcoma cells did not overexpress p53 (data not shown). Consistent with a poorly differentiated osteoblast phenotype, S1 cells expressed Runx2, alkaline phosphatase, type I collagen, osteopontin, and bone sialoprotein, but not osteocalcin (data not shown).

To further define behavior of the transformed cells in vivo, S1 cells were expanded in culture and infused into T-cell- and B-cell-deficient mice (NOD/SCID) intravenously (Fig. 5, top panels), intraperitoneally (Fig. 5, middle panels), and intramuscularly (Fig. 5, bottom panels). Within 3 weeks, all animals developed rapidly growing tumors, which were confined to the injected space (lung, peritoneum, or muscle). In addition, two animals developed muscular metastasis after i.v. infusion (Fig. 5, arrows, right top panel), thereby confirming the propensity of transformed cells to cause tumors in secondary recipients.

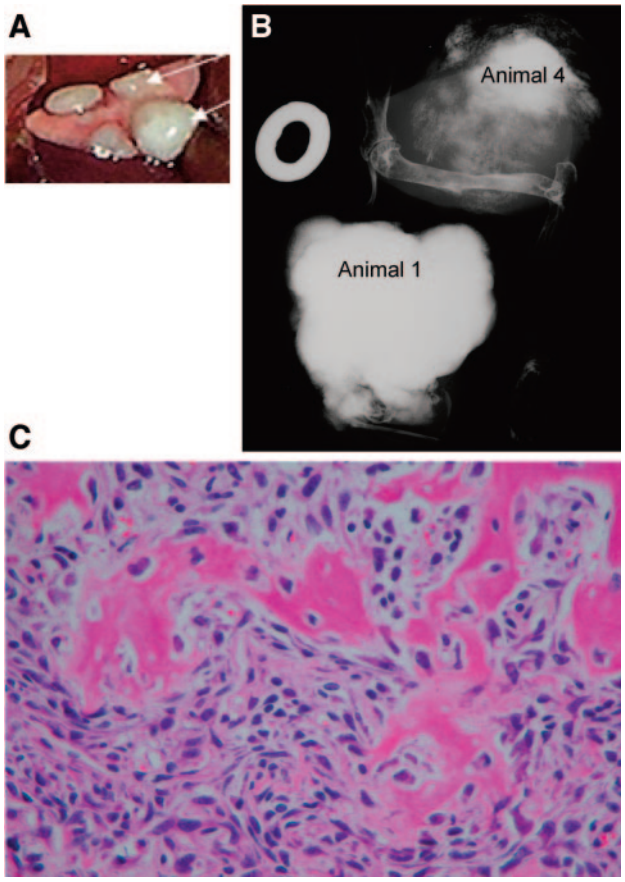

Figure 3. Sarcoma. **(A):** Ectopic ossicles were found on necropsy in the lungs of all animals that were infused with DsRed2 and luciferase positive and bone marrow transplantation (arrows; representative specimen). **(B):** Both extremity tumors were calcified on an x-ray image. **(C):** Tumors consisted of dense sheets and fascicles of spindloid cells with widespread deposition of a homogenous eosinophilic substance (osteoid) in a trabecular pattern, consistent with osteosarcoma. Hematoxylin-eosin stain. Magnification, ×400.

Genetic Events Associated with Sarcoma Transformation

Karyotype analysis of S1 and S2 sarcoma lines revealed multiple chromosomal abnormalities (Table 1; supplemental online Data 1), which were confirmed by FISH with SKY (data not shown). Nine of 15 karyotypic abnormalities were identified in both S1 and S2. Due to a possibility that emergence of MSC-derived cancer cells was related to transposon-mediated mutagenesis, we identified sites of transposition in the genomes of both S1 and S2 (supplemental online Table 1). None of the *luciferase* or *DsRed2* gene transpositions cloned to date occurred within a gene or a promoter of a gene with known osteogenic and/or proto-oncogene or tumor-suppressor gene capacity (supplemental online Data 2). Moreover, no common integration site was identified in S1 and S2. Because the SB transposon/transposase system can be used as an efficient tool for mammalian mutagenesis [29, 30], we sought to determine whether chromosomal instability of S1 and S2 was caused by genomic integration and persistent expression of transposase which could lead to remobilization and reinsertion of the transgene into new loci. There was no evidence of genomic integration or expression of SB transposase by western blotting in S1 and S2 cells (data not shown).

To further exclude the possibility that transposon-mediated mutagenesis was responsible for sarcoma transformation, we

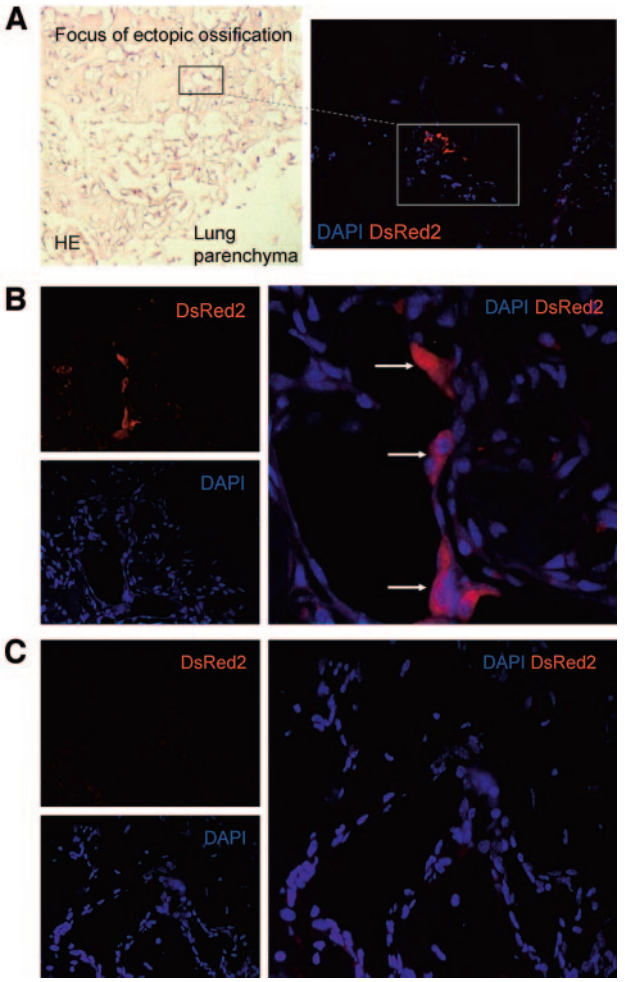

Figure 4. DsRed2 expression in sarcoma. **(A):** DsRed2$^+$ donor cells were identified within lung parenchyma. Magnifications, ×100 (left panel) and ×200 (right panel). **(B):** DsRed2 expression in sarcoma cells from animal 1, termed S1 (arrows). Magnifications, ×200 (left panels) and ×400 (merged image; right panel). **(C):** Lack of DsRed2 expression in sarcoma cells from animal 4, termed S2. Magnifications, ×200 (left panels) and ×400 (merged image; right panel). Abbreviations: HE, hematoxylin-eosin stain; DAPI, 4′,6-diamidino-2-phenylindole nuclear stain; DsRed2, native fluorescence.

studied the original MSC culture (not modified with transposons) for the presence of cytogenetic abnormalities. Cultured MSCs (passage 7, termed MSC-7) were found to be cytogenetically abnormal with two X chromosomes, two Y chromosomes, consistent loss of chromosome 7 and with two derivative chromosomes: der(3)t(3;), der(4)t(2;) (Fig. 6A; Table 1; supplemental online Data 1). These MSCs that had been cultured for 11 passages resulted in tumor formation when injected intravenously in C57BL/6 mice (three experiments, eight mice per experiment). Tumor occurrence was seen in the tail, limbs, and lungs of all injected recipients. Cells isolated from these tumors (termed B6-T1) revealed the existence of the original cell line karyotype and showed the existence of two new subclones (Fig. 6B; Table 1; supplemental online Data 1). Further clonal evolution in vivo was observed upon reinjection of the B6-T1 cells (tumor cells termed B6-T2) into secondary recipients. In addition to the main clone existing in the original MSC line and the B6-T1 subclones, further rearranged subclones were observed. In these subclones, dicentric chromosomes were observed (Fig. 6C; Table 1; supplemental online Data 1). In addition, both in B6-T1 and B6-T2, additional chromosome losses were seen involving several chromosomes resulting in peritriploid clones derived from a near tetraploid original line.

Cytogenetic Analysis and Assessment of Tumorigenicity of Additional Primary MSC Cultures

To study the extent to which the malignant transformation of MSCs was unique to this one MSC culture, new primary MSC cultures from C57BL/6 mouse BM were initiated. In one out of 10 additional cell cultures, we observed complex cytogenetic abnormalities at passage 5 with four X chromosomes, loss of chromosome 3 and 12, and with two derivative chromosomes: (der(4)t(4;7), der (7)t(3;7) (termed MSC-5; Table 1; supplemental online Fig. 4A). After i.v. injection of 1×10^6 passage 7 MSC-5 cells into C57BL/6 recipients ($n = 4$), no tumors were detected by 16 weeks after injection. These data indicate that the occurrence of genomic instability is not unique to the original MSC culture, but they also indicate that not all cytogenetically abnormal MSCs will cause sarcomas in vivo.

To determine whether cytogenetic abnormalities occurred uniquely in the C57BL/6 strain, MSC cultures were initiated from BALB/c mice. BALB/c primary MSC culture at passage 11 showed a loss of two copies of chromosome 13 in a tetraploid background and a derivative chromosome: der (4)t (4, 8) (termed B/c-11; Table 1; supplemental online Fig. 4B). These data indicate that the occurrence of genomic instability is not unique to the original MSC culture and that it is a mouse strain-independent event.

DISCUSSION

In the present study, we report the development of sarcomas in mice injected with ex vivo-expanded MSCs. In addition, primary BM-derived MSCs from two strains of mice exhibited cytogenetic changes after several passages in vitro. Although these cells did not form tumors upon in vivo injection, these data indicate that transformation is not uncommon after ex vivo expansion of MSCs. We hypothesize that sarcomas occur after prolonged in vitro expansion. Although the growth characteristics of human and murine MSCs are not identical [6, 31, 32] and murine cells are more prone to undergo immortalization and transformation in culture than human cells [33], these observations underscore the requirement for monitoring of human MSCs in clinical protocols.

Autologous MSCs may perhaps become tumorigenic [34, 35] and have been implicated in childhood leukemia [36], epithelial cancers [37], and osteogenic sarcoma [33, 38]. In addition, MSCs can synergize with other cell types in cancer evolution [39] and their immunomodulatory properties [40] can create a permissive environment for tumor growth in a murine melanoma model [41]. Transformation of murine MSCs into a malignant cell is not entirely unexpected, given the stem cell potential shared by cancer stem cells and MSCs [36, 42]. In addition, conditions of prolonged culture (4–5 months, as reported for human MSCs) [43] favor cells with rapid proliferation potential and minimal contact inhibition. It is striking, however, that even shorter term culture (12 weeks in the current study) was sufficient for the transformation of MSCs into a cell population with autonomous growth and biologic characteristics of sarcoma.

None of the identifiable SB transposition events occurred in a proto-oncogene or tumor-suppressor gene, nor was a common integration site identified in both S1 and S2 (supplemental online Table 1), and no identifiable integration event colocalized

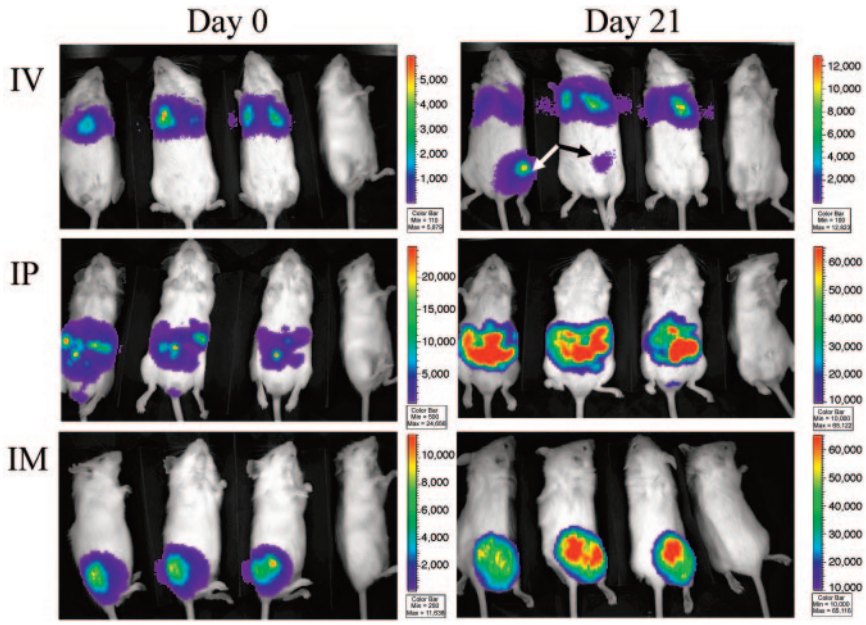

Figure 5. S1 cell line causes tumors in secondary recipients. S1 cells infused (dose: 10^6 per animal) into adult nonobese diabetic/severe combined immunodeficient mice expanded for a 21-day period and formed tumors after IV (top panels), IP (middle panels), and IM (bottom panels) delivery. Indicative of massive S1 proliferation, in vivo total-body photon emissions were extremely intense by day 21. Therefore, exposure time had to be decreased from 2 minutes on day 0 to 30 seconds after IV and to 1 second after IP and IM infusions on day 21. Abbreviations: IM, intramuscular; IP, intraperitoneal; IV, intravenous.

Table 1. Karyotypic abnormalities in MSC lines

Chromosome	S1	S2	MSC-7	B6-T1	B6-T2	MSC-5	B/c-11
1					der(1)t(X;1)		
2	−2	−2					
3	del(3)(F3)	del(3)(F3)	der(3)t(3;5)	der(3)t(3;5)	der(3)t(3;5)	−3	
4	der(4)t(2F1;4C4)		der(4)t(2;4)	der(4)t(2;4)	der(4)t(2;4)	der(4)t(4;7)	der(4)t(4;8)
5	der(5)dup(5)(DE2)del(5)(E2G2)	der(5)dup(5)(DE2)del(5)(E2G2)		del(5)	del(5)		
6	−6	−6					
7	−7, −7	−7, −7	−7,−7	−7,−7	−7, −7	der(7)t(3:7)	
8	del(8)(E1)	−8, −8					
9	−9, −9	−9, −9					
11	−11	−11, i(11)(q10)					
12	−12	−12				−12	
13		−13, −13		−13	−13		−13, −13
14	−14	−14					
16	−16	−16					
17							
18							
19			+19			+19	

Twenty metaphase cells were screened in each cell line.
Abbreviations: del, deletion; der, derivative; dup, duplication; i, isochromosome.

with chromosomal aberrations identified on karyotypes of S1 and S2 (Table 1). This does not entirely discount the possibility of insertional mutagenesis given that the genomic lesion may have occurred on the chromosome which was subsequently disrupted or lost. However, because of the common cytogenetic abnormalities found in different recipients as well as clonal evolution of the same MSC line (MSC-7; not labeled with transposons) after passage in murine recipients, we favor the explanation that genomic instability observed in both S1 and S2 resulted from a spontaneous unrepaired chromosomal lesion(s) that preceded the transposon insertion and led to transformation. This is further supported by cytogenetic clonal evolution of the same MSC line (MSC-7; not labeled with transposons) after passage in murine recipients.

Whereas several MSC cultures from separate donors, similar to the ones used in this report, remained euploid and showed no sign of accelerated proliferation or loss of contact inhibition in vitro, two other MSC cultures derived from two different mouse strains acquired cytogenetic abnormalities during passage. With respect to tumorigenicity risk of murine MSCs, this is difficult to quantify. However, aside from the single murine MSC culture that led to sarcomas characterized in this report, we were not able to reproduce the generation of sarcoma in more than 100 mice infused with MSCs at similar passages and doses as those that favored sarcoma formation, including the testing of murine MSCs that had cytogenetic abnormalities as described above. We speculate that, upon infusion of a relatively high number of MSCs, the initial clone may have encountered an environment that accelerated its selective and malignant growth culminating in complex unbalanced karyotypes with genomic amplification, numerical and structural abnormalities, which are all features of a subset of pleomorphic sarcomas, especially osteosarcomas [44, 45]. Whereas a large subset of primitive sarcomas is characterized by reciprocal translocations with a limited number of cytogenetic and/or molecular variants, pleomorphic sarcomas show highly complex karyotypes that often are genomically unstable in culture as well as in vivo. The sarcomagenesis displayed in the model system shown here is consistent with

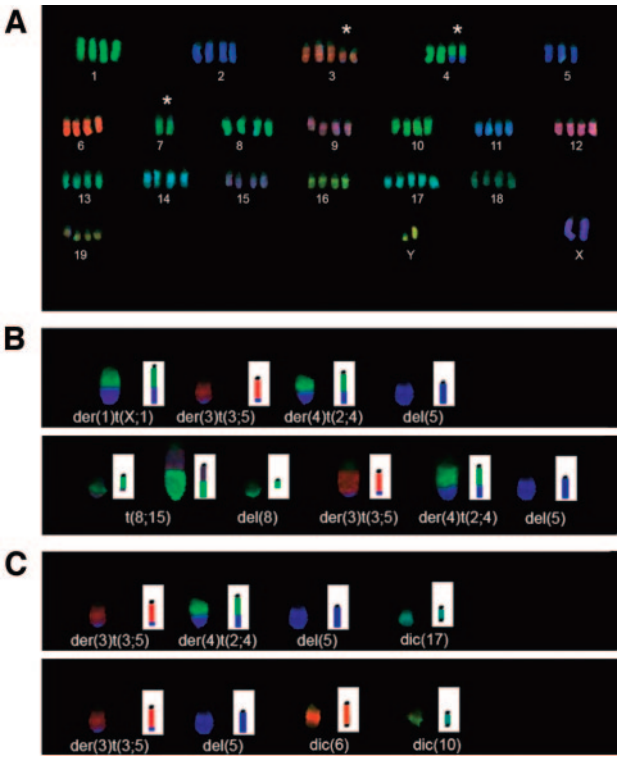

Figure 6. Clonal evolution of mesenchymal stem cell line (MSC-7) and tumor samples derived from it, B6-T1, and B6-T2. **(A):** Representative mouse combined binary ratio-fluorescence in situ hybridization karyogram of the MSC-7 cell line. Asterisks indicate the main recurrent alterations: der(3)t(3;5), der(4)t(2;4), and loss of chromosome 7. **(B):** Rearranged chromosomes of the two new clones occurred in the B6-T1 sample. Upper and lower panels show rearranged chromosomes of the two additional clones as compared with the main line (MSC-7). A schematic drawing of each derivative chromosome is shown in the insets; the black dots indicate the centromere of each derivative chromosome. **(C):** Rearranged chromosomes of two additional new clones occurred in B6-T2 cells derived from B6-T1. As in **(B)**, insets show schematic drawings of the derivative chromosomes.

latter pathway. This model is supported by additional experimental evidence of development of pleomorphic sarcomas in a multistep fashion as was shown recently in myxofibrosarcoma [46] or chondrosarcoma [47].

Sarcoma is related to MSCs by virtue of originating from mesenchymal cells. MSCs, however, are a heterogeneous population of BM cells, and it is therefore plausible that the transformed cell was not a true oligopotential MSC but a cell already committed to a specific (e.g., osteogenic) lineage. MSC DLs progressed from cells with osteogenic potential (initially trapped in lungs, where they formed foci of ectopic ossification in all animals) to cells with both osteogenic and malignant potential which metastasized and formed sarcomas in skeletal muscle and adjacent bone in two animals. The lung and muscle were both permissive sites for MSC DLs similar to sites observed in human sarcoma. The S1 cells have a rapid doubling time and express immature osteoblast markers consistent with the majority (75%) of human osteosarcomas [45].

To our knowledge, when compared with murine models of sarcoma with osteogenic potential described to date [48–51], the S1 is unique in being derived from C57BL/6 mice, in having a cytogenetic profile reminiscent of human osteosarcoma, and in being marked with both bioluminescent (*luciferase*) and fluorescent (*DsRed2*) genes. This latter capacity may be used in investigations of organ homing, cellular biodistribution, and dynamics of tumor response to chemotherapy and radiation in real time in vivo.

Conclusion

We describe transformation of murine MSCs into sarcoma. These findings underline the potential of MSCs for ectopic ossification and malignant transformation. In this context, our study highlights the importance of quality-control measures needed for ongoing and future clinical trials using human MSCs.

Acknowledgments

We thank Dr. David A. Largaespada for helpful comments, Dr. Chris Zurcher for histology slides, Andrew Price for lung testing, and Michael Goblirsch for x-ray imaging. The MSCs from C57BL/6 and several other mouse strains are available from the Tulane Center for Cell Therapy. E-mail requests to wolfe@tulane.edu. This work was supported by the Children's Cancer Research Fund (J.T.), The V Foundation for Cancer Research (J.J.W.), an award from the American Heart Association (M.J.O.), National Institutes of Health Child Health Research Scholar Award Grants 5K12-HD033692-10 (J.T.), RO1 AR48147 (J.J.W.), RO1 AR050074 (J.J.W.), T32 CA09138 (T.M.S.), AR48323 (D.J.P.), RO117447 (D.J.P.), RO1 HL55209 (B.R.B.), RO1 HL49997 (B.R.B.), National Center for Research Resources shared instrumentation Grant S10 RR16851, and the Netherlands Cancer Foundation (NKB 2004-3014).

J.T., A.J.N., W.E.F., and B.R.B. contributed equally to this work.

Disclosures

The authors indicate no potential conflicts of interest.

References

1 Friedenstein AJ, Chailakhjan RK, Lalykina KS. The development of fibroblast colonies in monolayer cultures of guinea-pig bone marrow and spleen cells. Cell Tissue Kinet 1970;3:393–403.

2 Ashton BA, Eaglesom CC, Bab I et al. Distribution of fibroblastic colony-forming cells in rabbit bone marrow and assay of their osteogenic potential by an in vivo diffusion chamber method. Calcif Tissue Int 1984;36:83–86.

3 Thomson BM, Bennett J, Dean V et al. Preliminary characterization of porcine bone marrow stromal cells: Skeletogenic potential, colony-forming activity, and response to dexamethasone, transforming growth factor beta, and basic fibroblast growth factor. J Bone Miner Res 1993;8:1173–1183.

4 Hurwitz DR, Kirchgesser M, Merrill W et al. Systemic delivery of human growth hormone or human factor IX in dogs by reintroduced genetically modified autologous bone marrow stromal cells. Hum Gene Ther 1997;8:137–156.

5 Pittenger MF, Mackay AM, Beck SC et al. Multilineage potential of adult human mesenchymal stem cells. Science 1999;284:143–147.

6 Peister A, Mellad JA, Larson BL et al. Adult stem cells from bone marrow (MSCs) isolated from different strains of inbred mice vary in surface epitopes, rates of proliferation, and differentiation potential. Blood 2004;103:1662–1668.

7 Zuk PA, Zhu M, Mizuno H et al. Multilineage cells from human adipose tissue: Implications for cell-based therapies. Tissue Eng 2001;7:211–228.

8 Wang JF, Wang LJ, Wu YF et al. Mesenchymal stem/progenitor cells in human umbilical cord blood as support for ex vivo expansion of CD34(+) hematopoietic stem cells and for chondrogenic differentiation. Haematologica 2004;89:837–844.
9 Lazarus HM, Koc ON, Devine SM et al. Cotransplantation of HLA-identical sibling culture-expanded mesenchymal stem cells and hematopoietic stem cells in hematologic malignancy patients. Biol Blood Marrow Transplant 2005;11:389–398.
10 Horwitz EM, Prockop DJ, Fitzpatrick LA et al. Transplantability and therapeutic effects of bone marrow-derived mesenchymal cells in children with osteogenesis imperfecta. Nat Med 1999;5:309–313.
11 Le Blanc K, Rasmusson I, Sundberg B et al. Treatment of severe acute graft-versus-host disease with third party haploidentical mesenchymal stem cells. Lancet 2004;363:1439–1441.
12 Jones OY, Steele A, Jones JM et al. Nonmyeloablative bone marrow transplantation of BXSB lupus mice using fully matched allogeneic donor cells from green fluorescent protein transgenic mice. J Immunol 2004;172:5415–5419.
13 Jones OY, Good RA, Cahill RA. Nonmyeloablative allogeneic bone marrow transplantation for treatment of childhood overlap syndrome and small vessel vasculitis. Bone Marrow Transplant 2004;33:1061–1063.
14 El-Badri NS, Maheshwari A, Sanberg PR. Mesenchymal stem cells in autoimmune disease. Stem Cells Dev 2004;13:463–472.
15 Studeny M, Marini FC, Dembinski JL et al. Mesenchymal stem cells: Potential precursors for tumor stroma and targeted-delivery vehicles for anticancer agents. J Natl Cancer Inst 2004;96:1593–1603.
16 Studeny M, Marini FC, Champlin RE et al. Bone marrow-derived mesenchymal stem cells as vehicles for interferon-beta delivery into tumors. Cancer Res 2002;62:3603–3608.
17 Ivics Z, Hackett PB, Plasterk RH et al. Molecular reconstruction of Sleeping Beauty, a Tc1-like transposon from fish, and its transposition in human cells. Cell 1997;91:501–510.
18 Bevis BJ, Glick BS. Rapidly maturing variants of the Discosoma red fluorescent protein (DsRed). Nat Biotechnol 2002;20:83–87.
19 Dupuy AJ, Clark K, Carlson CM et al. Mammalian germ-line transgenesis by transposition. Proc Natl Acad Sci U S A 2002;99:4495–4499.
20 Luo G, Ivics Z, Izsvak Z et al. Chromosomal transposition of a Tc1/mariner-like element in mouse embryonic stem cells. Proc Natl Acad Sci U S A 1998;95:10769–10773.
21 Yant SR, Meuse L, Chiu W et al. Somatic integration and long-term transgene expression in normal and haemophilic mice using a DNA transposon system. Nat Genet 2000;25:35–41.
22 Yant SR, Park J, Huang Y et al. Mutational analysis of the N-terminal DNA-binding domain of sleeping beauty transposase: Critical residues for DNA binding and hyperactivity in mammalian cells. Mol Cell Biol 2004;24:9239–9247.
23 Romeo S, Bovee JV, Grogan SP et al. Chondromyxoid fibroma resembles in vitro chondrogenesis, but differs in expression of signalling molecules. J Pathol 2005;206:135–142.
24 Szuhai K, Tanke HJ. COBRA: COmbined Binary RAtio labelling of nucleic acids probes for multi-colour FISH karyotyping. Nature Protocols 2006;1:264–275.
25 Telenius H, Carter NP, Bebb CE et al. Degenerate oligonucleotide-primed PCR: General amplification of target DNA by a single degenerate primer. Genomics 1992;13:718–725.
26 Telenius H, Pelmear AH, Tunnacliffe A et al. Cytogenetic analysis by chromosome painting using DOP-PCR amplified flow-sorted chromosomes. Genes Chromosomes Cancer 1992;4:257–263.
27 Szuhai K, Bezrookove V, Wiegant J et al. Simultaneous molecular karyotyping and mapping of viral DNA integration sites by 25-color COBRA-FISH. Genes Chromosomes Cancer 2000;28:92–97.
28 Schroeder TM, Kahler RA, Li X et al. Histone deacetylase 3 interacts with runx2 to repress the osteocalcin promoter and regulate osteoblast differentiation. J Biol Chem 2004;279:41998–42007.
29 Collier LS, Carlson CM, Ravimohan S et al. Cancer gene discovery in solid tumours using transposon-based somatic mutagenesis in the mouse. Nature 2005;436:272–276.
30 Dupuy AJ, Akagi K, Largaespada DA et al. Mammalian mutagenesis using a highly mobile somatic Sleeping Beauty transposon system. Nature 2005;436:221–226.
31 Lee RH, Hsu SC, Munoz J et al. A subset of human rapidly self-renewing marrow stromal cells preferentially engraft in mice. Blood 2006;107:2153–2161.
32 Munoz JR, Stoutenger BR, Robinson AP et al. Human stem/progenitor cells from bone marrow promote neurogenesis of endogenous neural stem cells in the hippocampus of mice. Proc Natl Acad Sci U S A 2005;102:18171–18176.
33 Prowse KR, Greider CW. Developmental and tissue-specific regulation of mouse telomerase and telomere length. Proc Natl Acad Sci U S A 1995;92:4818–4822.
34 Serakinci N, Guldberg P, Burns JS et al. Adult human mesenchymal stem cell as a target for neoplastic transformation. Oncogene 2004;23:5095–5098.
35 Prindull G, Zipori D. Environmental guidance of normal and tumor cell plasticity: Epithelial mesenchymal transitions as a paradigm. Blood 2004;103:2892–2899.
36 Greaves M. Molecular genetics, natural history and the demise of childhood leukaemia. Eur J Cancer 1999;35:1941–1953.
37 Houghton J, Stoicov C, Nomura S et al. Gastric cancer originating from bone marrow-derived cells. Science 2004;306:1568–1571.
38 Stark A, Aparisi T, Ericsson JL. Human osteogenic sarcoma: Fine structure of the osteoblastic type. Ultrastruct Pathol 1983;4:311–329.
39 Tabe Y, Konopleva M, Munsell MF et al. PML-RARalpha is associated with leptin-receptor induction: The role of mesenchymal stem cell-derived adipocytes in APL cell survival. Blood 2004;103:1815–1822.
40 Le Blanc K, Ringden O. Immunobiology of human mesenchymal stem cells and future use in hematopoietic stem cell transplantation. Biol Blood Marrow Transplant 2005;11:321–334.
41 Djouad F, Plence P, Bony C et al. Immunosuppressive effect of mesenchymal stem cells favors tumor growth in allogeneic animals. Blood 2003;102:3837–3844.
42 Warner JK, Wang JC, Hope KJ et al. Concepts of human leukemic development. Oncogene 2004;23:7164–7177.
43 Rubio D, Garcia-Castro J, Martin MC et al. Spontaneous human adult stem cell transformation. Cancer Res 2005;65:3035–3039.
44 Mitelman F. Recurrent chromosome aberrations in cancer. Mutat Res 2000;462:247–253.
45 Gorlick R, Anderson P, Andrulis I et al. Biology of childhood osteogenic sarcoma and potential targets for therapeutic development: Meeting summary. Clin Cancer Res 2003;9:5442–5453.
46 Willems SM, Debiec-Rychter M, Szuhai K et al. Local recurrence of myxofibrosarcoma is associated with increase in tumour grade and cytogenetic aberrations, suggesting a multistep tumour progression model. Mod Pathol 2006;19:407–416.
47 Bovee JV, Cleton-Jansen AM, Taminiau AH et al. Emerging pathways in the development of chondrosarcoma of bone and implications for targeted treatment. Lancet Oncol 2005;6:599–607.
48 Khanna C, Prehn J, Yeung C et al. An orthotopic model of murine osteosarcoma with clonally related variants differing in pulmonary metastatic potential. Clin Exp Metastasis 2000;18:261–271.
49 Bell RS, Roth YF, Gebhardt MC et al. Timing of chemotherapy and surgery in a murine osteosarcoma model. Cancer Res 1988;48:5533–5538.
50 Dunn TB, Andervont HB. Histology of some neoplasms and non-neoplastic lesions found in wild mice maintained under laboratory conditions. J Natl Cancer Inst 1963;31:873–901.
51 Choi CH, Sedlacek RS, Suit HD. Radiation-induced osteogenic sarcoma of C3H mouse: Effects of Corynebacterium parvum and WBI on its natural history and response to irradiation. Eur J Cancer 1979;15:433–442.

See www.StemCells.com for supplemental material available online.